Trajectory pattern recognition in video microscopy of *Trypanosoma cruzi* parasites

Geovani L. Martins
Postgraduate Program in Computer Science
Federal University of Ouro Preto
Minas Gerais, Brazil
Email: geovani.martins@aluno.ufop.edu.br

***Abstract*—The visual field captured in video microscopy can reveal challenging dynamic patterns for computer vision techniques. In the parasitological analysis of *Trypanosoma cruzi*, blood cells and parasites perform characteristic motions (collateral, fluctuating and PTZ). Introduced in a recent work, the aim of this study is to present details about the related motion patterns. The identification of these patterns can reveal interesting aspects of dynamicity in optical microscopy video. For this, we propose the analysis of features extracted directly from trajectory segments to build a classification model with the Random Forest algorithm.**

I. Introduction

While observing samples infected with *Trypanosoma cruzi* (*T. cruzi*) parasites, the etiologic agent of Chagas disease [1], the parasitologist can see several artifacts that move under the microscope's visual field. Blood cells and parasites form a challenging dynamic context for computer vision approaches aimed at detecting hemoflagellate parasites [2]. Figure 1 shows the motion patterns that can be observed in *T. cruzi* parasitological analyzes.

Collateral motion corresponds to stimuli perceived during *T. cruzi* locomotion, which interacts with neighboring cells and fluids. It is not the parasite's intrinsic motion but a motion resulting from collisions with other artifacts in the scene. Naturally, the parasite changes the characteristics of its motion in the presence of cells [3].

Fluctuating motion is mostly identified in cells that are suspended in the blood sample. Although cells do not have natural motion, they are susceptible to external actions that make them vulnerable to sudden motion. An example of this is the handling of moving parts of the microscope that can destabilize the cells during the inspection.

PTZ (pan–tilt–zoom) motion is related to the focus adjustments of the microscope lenses or even the camera that captures the visual field. In this case, static artifacts can express apparent motion from the focus adjustments. Generally, this type of motion influences the performance of computational approaches that extract spatio-temporal features of the scene.

The dynamic context involved in the computational detection of *T. cruzi* in blood optical microscopy videos still lacks studies that demonstrate the motion patterns introduced in previous works. Thus, the main contribution of this work is to develop an approach that allows the recognition of related motion patterns (collateral, fluctuating, and PTZ). Our hypothesis is that the analysis of the trajectories of parasites and blood cells present in optical microscopy videos makes it possible to recognize dynamic patterns. A consequence of this study would be the identification of motile artifacts in these scenes based on the analysis of their trajectory.

II. Related work

Trajectory mining allows for the discovery of interesting patterns in databases, sometimes unexpected [4], [5]. Recently, some works have been published to recognize trajectory patterns in various applications, such as environment and energy [6], urban planning [7], traffic [8], but we do not know approaches directed to trajectories extracted from blood optical microscopy videos obtained in parasitological analyses.

The identification of trajectory patterns can occur from two approaches: clustering or classification.

A. Clustering

It is an unsupervised learning process that reveals similarities within a trajectory dataset by dividing trajectories into categories (i.e., clusters) according to their properties. A common approach is to represent trajectories as a feature vector and thus measure the similarity between the vectors [4]. However, trajectories can vary in terms of length, shape, sampling, number of points and other properties, which makes it difficult to work with this representation. Some approaches are applicable to entire trajectories [9], [10]. However, more works have focused on discovering sub-trajectories, which allows finding patterns in certain parts of them [11]. Lee et al. (2007) proposed a partition-and-group framework, which partitions an entire trajectory into a set of line segments, and groups similar line segments into a cluster using the Trajectory Hausdorff Distance [12].

B. Classification

Classification is a supervised or partially supervised learning process. The classification classes need to be predefined, and a training set of objects needs to be prelabeled with the class that they belong to. A typical trajectory classification algorithm contains two steps. First, it needs to extract a set of discriminative features that can be used to train an existing standard classification model (e.g., random forest, support vector machine (SVM) and nearest neighbors). The second step is

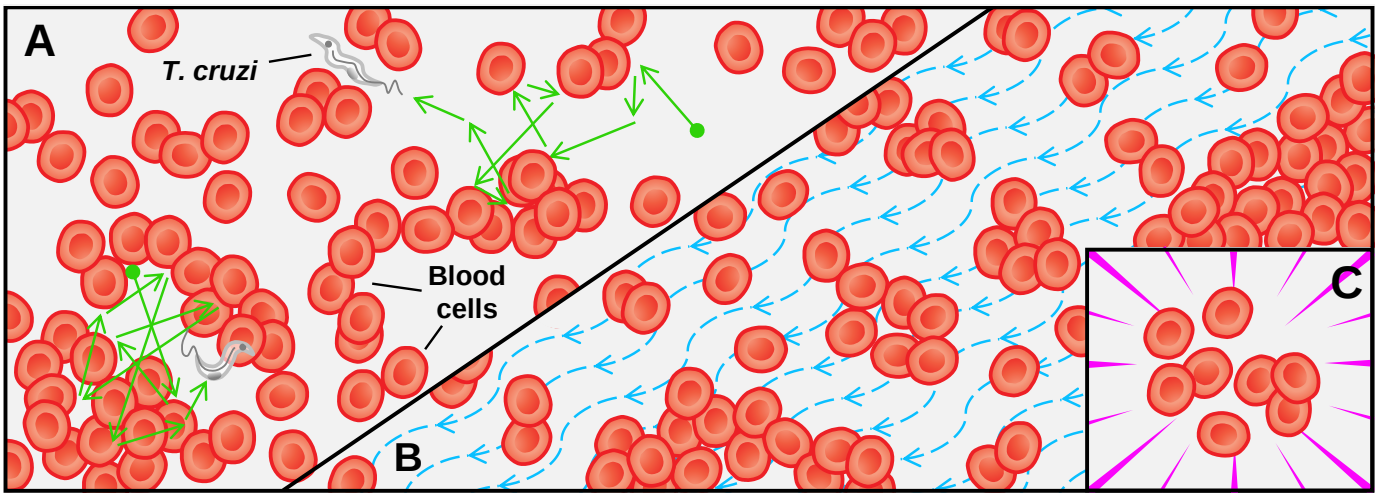

Fig. 1. Dynamism in video microscopy of *T. cruzi* parasites. Three motions are illustrated: (A) collateral; (B) fluctuating and (C) PTZ.

to select a proper standard classification model, and then, apply it to the extracted discriminative features. Bolbol et al. (2012) utilized SVMs for transportation mode classification. Zheng et al. (2010) did similar work, except that ~~that~~ they applied a decision tree-based inference model. In many situations, trajectories are classified following some preprocessing (e.g., segmentation, clustering, statistical analysis) that prepares the features needed for classification [13].

III. Methodology

Our study uses trajectories of artifacts observed in video microscopy of *T. cruzi* parasitological analysis. Figure 2 shows an overview of the approach, in which we build and train a model to recognize dynamic patterns in trajectories. The model was tested with new trajectory segments, where we evaluated its predictive performance. We present the steps involved in training and testing experiments in more detail below.

A. Dataset

The trajectories were obtained from blood optical microscopy videos by Martins et al. (2021). These videos correspond to laboratory inspections of *T. cruzi*, in which the trypomastigote form of the parasite can be seen. In general, the videos are up to 10 seconds long. The frame rate is approximately 30 frames per second (fps), and the resolution is 640 x 480 pixels.

We know the trajectories of parasites in work by Martins et al. (2021). However, cell trajectories are not labeled. In this case, we randomly choose some cells to investigate fluctuating and PTZ motion patterns. We generate three cell trajectories for each parasite in the videos. For this, we use the same parasites trajectory labeling tool [14]. An expert validated the trajectories obtained. Table I shows a summary of the dataset.

The trajectory of an artifact in the scene can be described:

$$traj =< p_1, p_2, p_3, ..., p_n >, \quad (1)$$

where

TABLE I
Trajectory Dataset Details

	Video	Parasite trajectories	Cell trajectories	Total frames	Duration (s)
Train	P1	1	3	325	10
	P2	1	3	269	8
	P3	1	3	255	8
	P4	1	3	200	6
	P5	1	3	267	8
	P6	1	3	202	6
	P7	1	3	184	6
	P8	1	3	189	6
	P9	2	6	313	10
	P10	3	9	310	10
Test	V1	3	9	74	4
	V2	1	3	245	8
	V3	3	9	160	5

$$p_n = (x_n, y_n, t_n), \quad (2)$$

is the *n*th trajectory point, that is, the point in a given video frame. The (x_n, y_n) coordinate is the spatial location of p_n in video pixels and t_n is the time at which the point was regularly recorded.

B. Segmentation

Table I shows that the trajectories have different lengths due to the number of video frames. In addition, our dataset is unbalanced because of the established criterion of three cell trajectories for each parasite trajectory. Certainly, this can be a problem for building a trajectory classification model based on machine learning algorithms. Thus, we propose the segmentation of trajectories to avoid a biased model for trajectory classes with more observations.

Our segmentation consists of different cut points on a given trajectory to obtain several segments or sub-trajectories. Therefore, a trajectory segment can be described as follows:

$$traj_{seg} =< p_{i+1}, p_{i+2}, p_{i+3}, ..., p_{i+k} >, \quad (3)$$

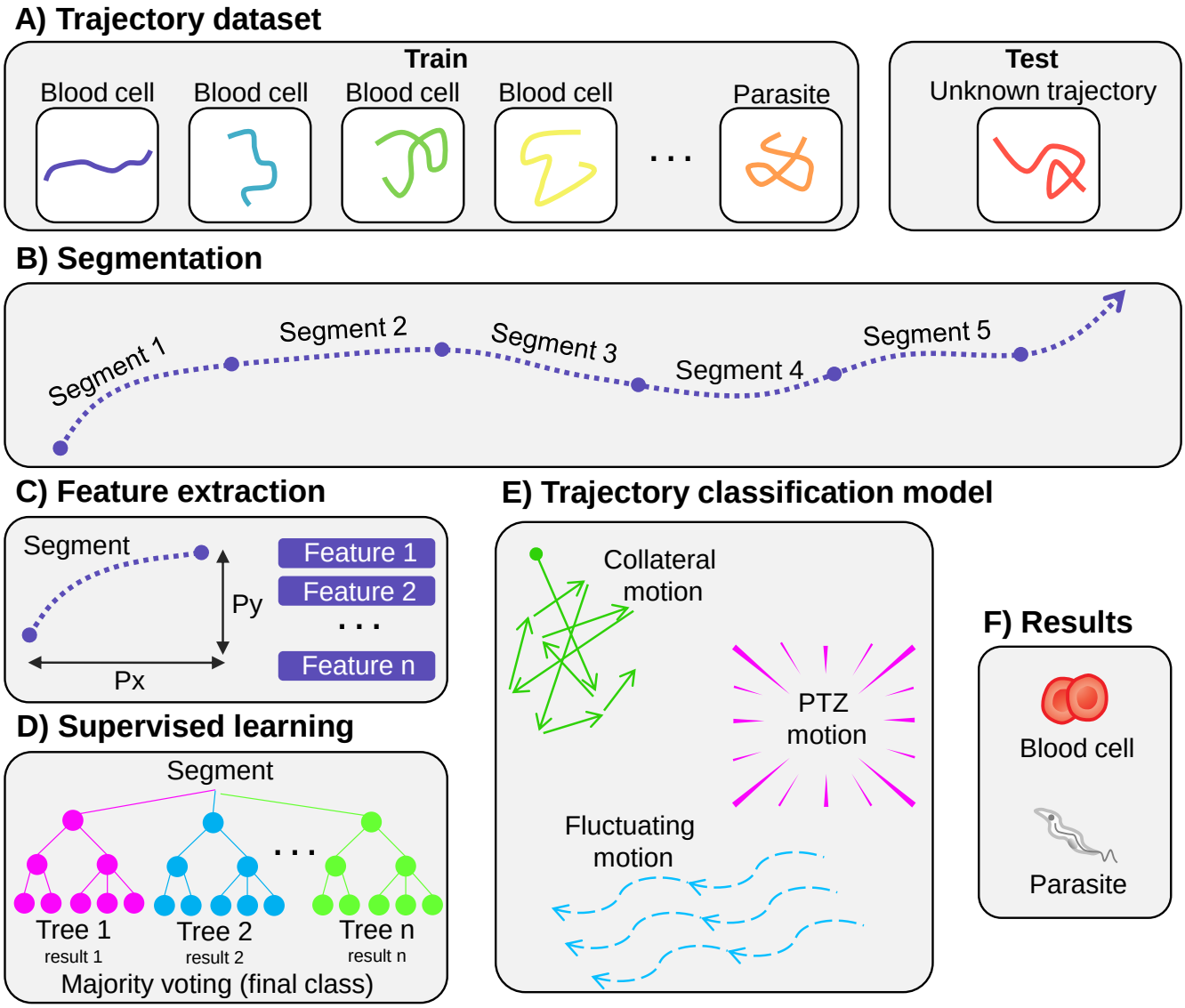

Fig. 2. A schematic representation of the proposed approach. (A) Trajectory dataset; (B) segmentation; (C) feature extraction; (D) supervised learning; (E) trajectory classification model and (F) results. The training flow corresponds to steps A-D. The test flow comprises steps A, B, C, E and F, respectively.

where i is the cutoff point on the trajectory and k is the total of points to be considered in the segment.

Note that each segment has successive points according to the sequence of video frames.

C. Feature extraction

Features are extracted directly from trajectory segments. We characterize the segments by their mean speed and mean squared displacement. We also considered a dispersion measure that could highlight aspects of trajectory morphology, so we calculated the spectral entropy.

1) Mean speed: The mean artifact speed along a single trajectory segment consisting of k points is:

$$\bar{v} = \frac{1}{k-1} \sum_{i=1}^{k-1} \frac{\sqrt{(x_{i+1} - x_i)^2 + (y_{i+1} - y_i)^2}}{\Delta t}. \quad (4)$$

Since the videos were taken at 30 fps, then:

$$\Delta t = t_{i+1} - t_i = 0.033s. \quad (5)$$

2) Mean squared displacement (MSD): The MSD can be computed as follows for a trajectory segment consisting of k points:

$$MSD(t_j) = \frac{1}{k-j} \sum_{i=1}^{k-j} (x_{i+j} - x_i)^2 + (y_{i+j} - y_i)^2, \quad (6)$$

where $t_j = j\Delta t$.

3) Spectral entropy: Spectral entropy is obtained for the x and y coordinates separately. It is defined to be the Shannon entropy [15] of the power spectral density (PSD) [16] of the data:

Just a question:
These three features are able to identify each segment?
Or you pretend to generate other types of features?
Of course, you'll have the answers after the tests, but it's only a questioning...lol....

$$H(x, f_s) = -\sum_{f=0}^{f_s/2} P(f) \log_2[P(f)], \tag{7}$$

where P is the normalised PSD, and f_s is the sampling frequency.

D. Classification

We used the random forest algorithm [17], [18] to build the model. A random forest algorithm consists of many decision trees. The forest generated by the random forest algorithm is trained through bagging or bootstrap aggregating. Bagging is an ensemble meta-algorithm that improves the accuracy of machine learning algorithms.

A decision tree consists of three components: decision nodes, leaf nodes, and a root node. A decision tree algorithm divides a training dataset into branches, which further segregate into other branches. This sequence continues until a leaf node is attained. The leaf node cannot be segregated further.

The nodes in the decision tree represent attributes that are used for predicting the outcome. Decision nodes provide a link to the leaves. The following diagram shows the three types of nodes in a decision tree. you didn't put the diagram

After constructing the trajectory classification model, a new test trajectory segment can be analyzed. If the pattern is similar to collateral motion, the artifact is classified as a parasite. If the segment presents a PTZ or fluctuating motion pattern, it is classified as a blond cell.

E. Metrics

The evaluation of the model will be carried out with the following metrics:

$$Precision = \frac{True\ Positive}{True\ Positive + False\ Positive} \tag{8}$$

$$Recall = \frac{True\ Positive}{True\ Positive + False\ Negative} \tag{9}$$

$$F_\beta = \frac{(\beta^2 + 1) \times Precision \times Recall}{\beta^2 \times Precision + Recall}, (0 \leq \beta \leq +\infty) \tag{10}$$

We set $\beta = 1$. Therefore, F_1 equals the harmonic mean between *precision* and *recall*, emphasizing which value is less.

References

[1] J. A. Pérez-Molina and I. Molina, "Chagas disease," *The Lancet*, vol. 391, no. 10115, pp. 82–94, 2018.

[2] G. L. Martins, D. S. Ferreira, and G. L. B. Ramalho, "Collateral motion saliency-based model for *Trypanosoma cruzi* detection in dye-free blood microscopy," *Comput. Biol. Med.*, vol. 132, p. 104220, May 2021.

[3] J. A. Arias-del Angel, J. Santana-Solano, M. Santillán, and R. G. Manning-Cela, "Motility patterns of trypanosoma cruzi trypomastigotes correlate with the efficiency of parasite invasion in vitro," *Scientific Reports*, vol. 10, no. 1, pp. 1–11, 2020.

[4] Y. Zheng, "Trajectory data mining: An overview," *ACM Trans. Intell. Syst. Technol.*, vol. 6, no. 3, May 2015. [Online]. Available: https://doi.org/10.1145/2743025

[5] D. Wang, T. Miwa, and T. Morikawa, "Big trajectory data mining: A survey of methods, applications, and services," *Sensors*, vol. 20, no. 16, 2020. [Online]. Available: https://www.mdpi.com/1424-8220/20/16/4571

[6] J. Shang, Y. Zheng, W. Tong, E. Chang, and Y. Yu, "Inferring gas consumption and pollution emission of vehicles throughout a city," in *Proceedings of the 20th ACM SIGKDD International Conference on Knowledge Discovery and Data Mining*, ser. KDD '14. New York, NY, USA: Association for Computing Machinery, 2014, p. 1027–1036. [Online]. Available: https://doi.org/10.1145/2623330.2623653

[7] N. Shahraki, H. Cai, M. Turkay, and M. Xu, "Optimal locations of electric public charging stations using real world vehicle travel patterns," *Transportation Research Part D: Transport and Environment*, vol. 41, pp. 165–176, 2015. [Online]. Available: https://www.sciencedirect.com/science/article/pii/S1361920915001352

[8] K. Soltani Naveh and J. Kim, "Urban trajectory analytics: Day-of-week movement pattern mining using tensor factorization," *IEEE Transactions on Intelligent Transportation Systems*, vol. 20, no. 7, pp. 2540–2549, 2019.

[9] S. Gaffney and P. Smyth, "Trajectory clustering with mixtures of regression models," in *Proceedings of the Fifth ACM SIGKDD International Conference on Knowledge Discovery and Data Mining*, ser. KDD '99. New York, NY, USA: Association for Computing Machinery, 1999, p. 63–72. [Online]. Available: https://doi.org/10.1145/312129.312198

[10] J. Alon, S. Sclaroff, G. Kollios, and V. Pavlovic, "Discovering clusters in motion time-series data," *2003 IEEE Computer Society Conference on Computer Vision and Pattern Recognition, 2003. Proceedings.*, vol. 1, pp. I–I, 2003.

[11] M. Y. Ansari, Mainuddin, A. Ahmad, and G. Bhushan, "Spatiotemporal trajectory clustering: A clustering algorithm for spatiotemporal data," *Expert Systems with Applications*, vol. 178, p. 115048, 2021. [Online]. Available: https://www.sciencedirect.com/science/article/pii/S0957417421004899

[12] J. Chen, M. K. Leung, and Y. Gao, "Noisy logo recognition using line segment hausdorff distance," *Pattern Recognit.*, vol. 36, pp. 943–955, 2003.

[13] R. Saini, P. Kumar, P. P. Roy, and U. Pal, "Modeling local and global behavior for trajectory classification using graph based algorithm," *Pattern Recognition Letters*, vol. 150, pp. 280–288, 2021. [Online]. Available: https://www.sciencedirect.com/science/article/pii/S0167865519301631

[14] D. Brown, "Tracker: Video analysis and modeling tool," 2009, accessed in November 2021. [Online]. Available: https://physlets.org/tracker/

[15] T. Inouye, K. Shinosaki, H. Sakamoto, S. Toi, S. Ukai, A. Iyama, Y. Katsuda, and M. Hirano, "Quantification of eeg irregularity by use of the entropy of the power spectrum," *Electroencephalography and Clinical Neurophysiology*, vol. 79, no. 3, pp. 204–210, 1991. [Online]. Available: https://www.sciencedirect.com/science/article/pii/001346949190138T

[16] C. E. Shannon, "Communication in the presence of noise," *Proceedings of the IRE*, vol. 37, no. 1, pp. 10–21, 1949.

[17] L. Breiman, "Random forests," *Machine learning*, vol. 45, no. 1, pp. 5–32, 2001.

[18] N. M. Abdulkareem, A. M. Abdulazeez *et al.*, "Machine learning classification based on radom forest algorithm: A review," *International Journal of Science and Business*, vol. 5, no. 2, pp. 128–142, 2021.